



Anal. Bioanal. Chem. Res., Vol. 6, No. 1, 183-193, June 2019.

Titanium Dioxide Nanofibers Decorated Nickel Nanoparticles as Effective Electrocatalyst for Urea Oxidation

M. Mazloum-Ardakani*, M. Yavari and A. Khoshroo

Department of Chemistry, Faculty of Science, Yazd University, Yazd, 89195-741, Iran

(Received 9 March 2018 Accepted 13 November 2018)

In this work, for the first time, a novel construction procedure for urea oxidation based on titanium dioxide (TiO₂) nanofibers (NFs) decorated Ni nanoparticles (NiNPs) is reported. Nickel nanoparticles were electrodeposited on the surface of titanium dioxide nanofibers (TNF-NiNPs) and the resulting modified electrode was characterized by scanning electron microscopy (SEM). Urea electro-oxidation reaction in NaOH solution on (TNF-NiNPs) as the electrode is studied by cyclic voltammetry (CV) and chronoamperometry (CA) methods. The surface coverage of TNF-NiNPs /GC electrode was calculated to be $\Gamma_a^* = 4.16 \times 10^{-7}$ mol cm², which is higher than corresponding value reported for the urea biosensor using Ni matrix. The electrochemical results showed that the presented electrode is effective and has a good electrocatalytic activity for urea oxidation and the structures of nanofibers have great effect on the electrooxidation of urea.

Keywords: Urea electrooxidation, Electrospinning, Nickel nanoparticles, Titanium dioxide nanofiber

INTRODUCTION

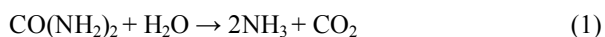
The improvement of nanotechnology has been increasing along the last years and nanostructured materials have important consideration due to their unique properties [1,2]. Nanomaterials are used in solar cells [3], catalysis [4], and sensors and biosensors [5] among these nanomaterials, nickel nanoparticles has been widely studied because of their application in batteries and electrocatalysis electrodes [6-9]. Nickel and nickel materials compared to precious metals are proper for electrochemical energy related and electrochemical analysis research works. These materials are puissant of replacing platinum based electrodes due to the excellent catalytic abilities of nickel-based electrodes, those involving glucose [7,9], oxygen [10], alcohols [11] and urea [12]. Different materials such as Nobel metals, non-Nobel metals and etc were used to electrooxidation of urea. Noble metals (Pd, Pt, Rh) are good based electrodes to catalyst hydrogen peroxide and alcohol [13], not for urea [14,15]. Noble metals can use in acidic

medium not in alkaline medium because alkaline medium has low corruptive and are expensive. Among non-Nobel metals, Botte *et al.* [14,16-19] find out nickel demonstrate lower oxidation potentials and higher current for the electro-oxidation of urea hence non-noble metals are suitable electrocatalyst for the electro-oxidation of urea in alkaline medium. Some reports been have been published on a nickel nanoribbons [20], nickel-carbon sponge [21], nickel nanowires [22,23].

Urea (CO(NH₂)₂) concentration in medical field is important, where above or below in its concentration can be communicated to liver and kidney sickness. Allowable level of urea concentration in serum is about 2.5-6.7 mM. This concentration of urea 30-80 mM causes some sickness such as renal inadequacy. At this level, hemolysis should be done [24,25]. Different technique such as amperometry and potentiometry have been proposed, for diagnosis of urea [26], but low cost and simplest techniques with easy operation to produce hydrogen from urea electrolysis are needed [27]. The electrochemical oxidation of urea has a lot of attention because the electrolysis of urea including solutions may be substitute to the electrolysis of water

*Corresponding author. E-mail: mazloum@yazd.ac.ir

[14,23,28-30]. Standard cell voltage for production of hydrogen through water electrolysis is 1.23 V, but through urea electrolysis is 0.37 V, is lower than water electrolysis [14]. Urea in the waste water not only can motive water and oil contamination but also can create humans and air contamination problems. In other words, the untreated urea rich wastewater has negative influence on the environment, it can be easily fragmented to ammonia and carbon dioxide and releases to the air according to this reaction [31].



The ammonia can be oxidized to hazardous compounds such as nitrites, nitrates and nitric oxides. The ammonia can be dissolved in to the rain and lead to acid rain pollution and have negative effects on the plants, buildings, soil, *etc.* Because of the bad urea decomposition in urine and generate hydrogen fuel simultaneously, urine electrolysis to hydrogen fuel can be happened [14]. This significance can be deployment to the order of urea that including industrial waste streams. Hence the measurement and decomposition of urea are important [32].

The nanostructured titania (TiO_2) is used in sensors, catalysis, solar cell and high performance photovoltaics because of the uniform structure, high specific surface area and chemical durability [33-35]. One dimensional (1D) nanomaterials such as nanofibers, nanowires, nanotubes, *etc.* can increase mass transition and remarkable in the sensing signal [36,37]. 1D nanofibers cause the higher diffusion of redox species due to its electrocatalytic activity, great electron transfer properties and mechanical strength [33,38,39]. Because of the small isoelectric point of TiO_2 , steady stick of biomolecules for functionalization is not possible, hence TiO_2 nanofibers for biosensing are used for few analytes such as glucose and urea [40-42]. TiO_2 nanoparticles, nanofibers and nanotubes are usually prepared by different methods such as template growth [43], sol-gel [44] and electrospinning technique [45] *etc.*

Electrospinning is the simplest and new method for synthesis of nanofibers with different diameters and morphologies at room temperature. Tension, viscosity, surface and the density of net charges of the solution can affect the morphology of nanofiber [46].

In the present work, we investigated a novel non-

enzymatic electrode based on TiO_2 nanofiber and Ni nanoparticles (TNF/NiNPs) deposited on glassy carbon electrode that was used for electro-oxidation of urea. Results illustrate that offered electrode showed high activity and good stability. Presence and structure of nanofiber has great effect on electro-oxidation of urea because of the big axial ratio of the nanofibers increases the electrons transfer via the catalyst material. Hence TiO_2 nanofibers are good support for electrodeposit of NiNPs.

EXPERIMENTAL

Chemicals and Apparatus

The electrochemical measurements were performed with a Zive lab potentiostat/galvanostat. A three-electrode system was used, where a glassy carbon (GC) electrode as the working electrode, a platinum wire as the counter electrode and saturated calomel electrode (SCE) as the reference electrode. An electrospinning device, Fanavaran Nano-Meghyas Model: ES1000 with controllable feeding rate and DC voltage range of 5-30 kV was used to fabricate nanofiber.

TiO_2 nanofibers were synthesized in our previous work [46] by acetic acid, titanium tetraisopropoxide (TTIP), polyvinylpyrrolidone (PVP) and urea, from Merck (Darmstadt, Germany) with analytical grade.

Preparation of the Electrode

Ni nanoparticle was synthesized by electrochemical method [47]. To get the best situation in the preparation of TNF-NiNPs/GC electrode, at first, the surface of GC electrode was polished on a polishing cloth with 0.05 mm alumina powder and then washed thoroughly with double distilled water. GCE was created with Ni nanoparticle and TiO_2 nanofiber. We optimized the time, amount of the NiNPs and TiO_2 NF that were loading on the surface of the electrode (Fig. 1).

First, about 2.0 mg of nanofibers were dispersed in 0.45 ml ethanol, 0.45 ml water and 100 μl nafion in an ultrasound bath for 30 min. Then a volume of 3.0 μl of the suspension was applied directly on a GC electrode surface and dried in air, then the potentiostatic deposition of nickel nanoparticle on the TNF-GCE from an aqueous solution of 60 mM Ni^{2+} by controlled potential coulometry (CPC)

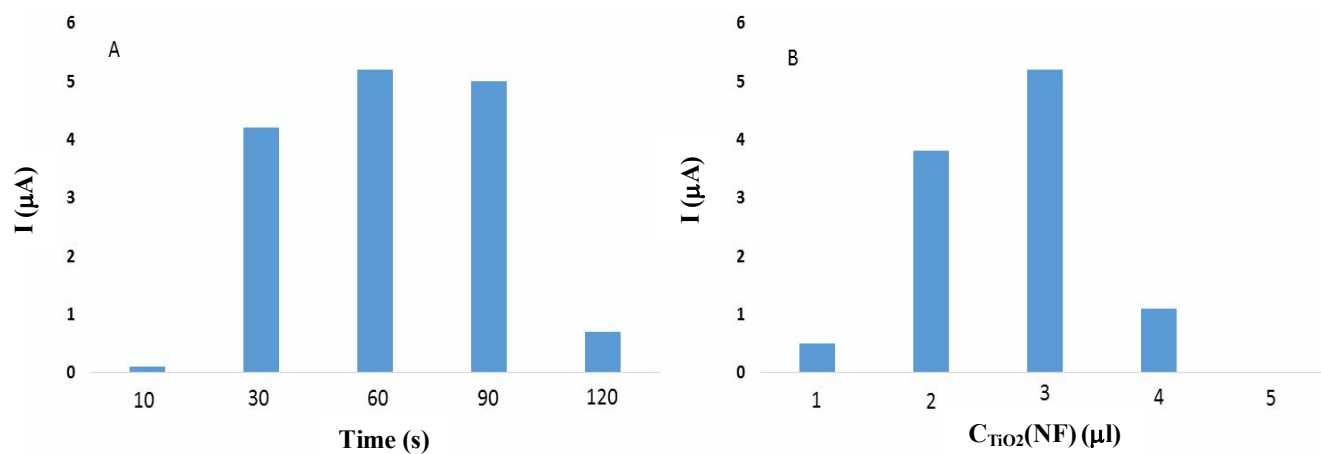


Fig. 1. Optimized situation of loading NiNPs and TiO_2 NF. (A) Optimized time for deposited NiNPS vs. I. (B) optimized concentration of TiO_2 NF vs. I at scan rate 0.15 V s^{-1} .

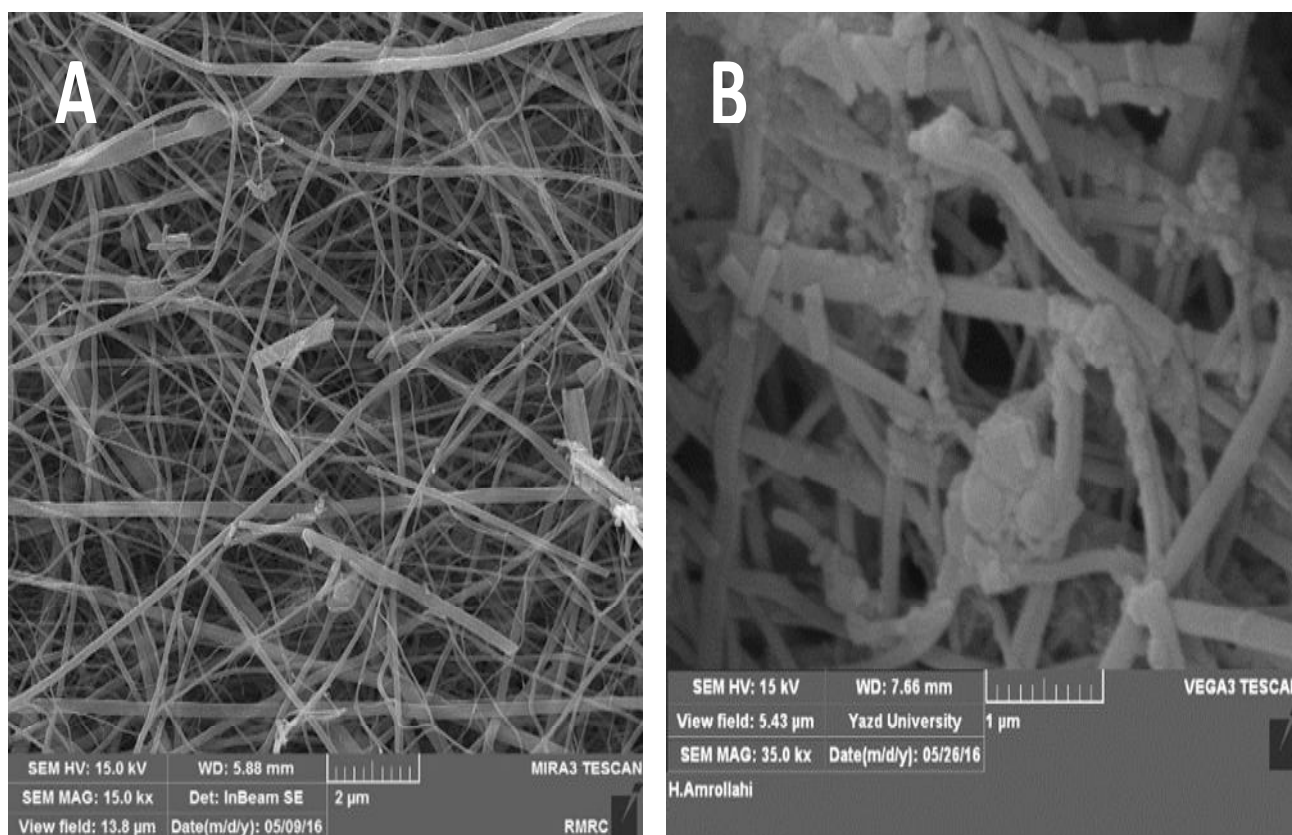


Fig. 2. SEM images of TiO_2 nanofibers (A) and TNF-NiNPs (B).

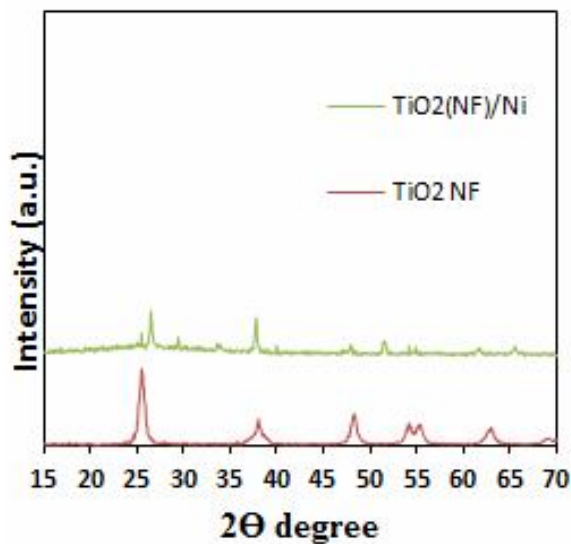


Fig. 3. XRD patterns of the TiO₂ NFs, TiO₂@C NFs, TiO₂ NFs-Ni and TiO₂@C NFs-Ni.

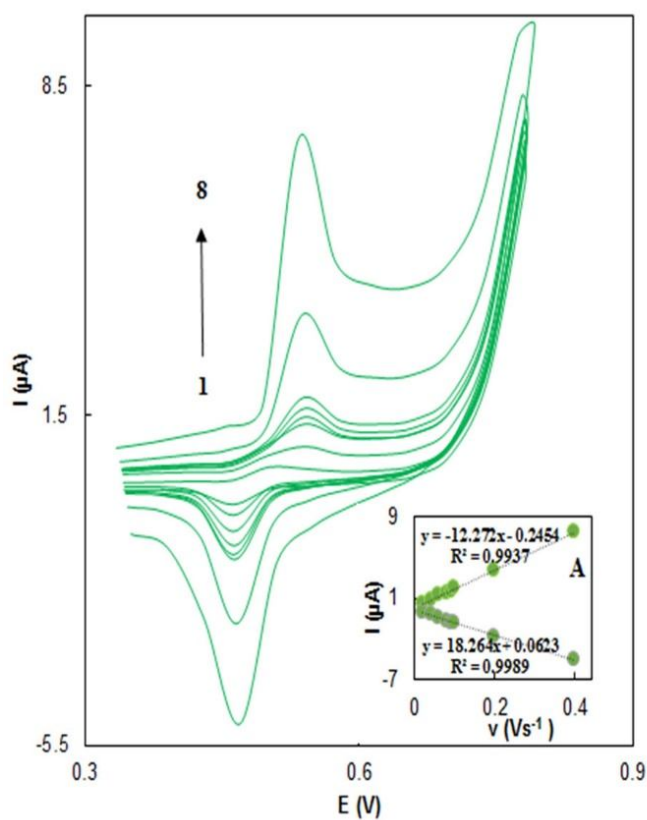


Fig. 4. CVs of the TiO₂ (NF) /NiNPs electrode in 1 M NaOH at different scan rates: 0.02, 0.04, 0.06, 0.08, 0.09, 0.1, 0.2 and 0.4 V s⁻¹ from 1 to 6, respectively. Inset (A) Plots of peak current *versus* scan rate.

applying a constant potential electrolysis at -0.6 V for 60 s [7].

RESULTS AND DISCUSSION

Characterization of TNF -NiNPs

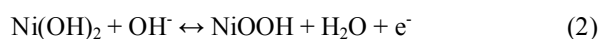
The morphology of TNF-NiNPs was studied by scanning electron microscopy (SEM) and X-Ray diffraction (XRD) patterns.

Figures 2A and B shows SEM image of TiO₂ (NF) and TNF-NiNPs that was utilized to study the surface of materials. We can see that the fibrous structure nanofibers with clear surface and deposit the NiNPs on the TNF changes the morphology. The images were get at low (A, B) and high magnification (inset B). Enhancing the magnification, the nanostructured nature of the fibers is clearly observed, and it could be seen that at the surface of TNF-NiNPs the Ni nanoparticles are uniformly deposited.

The X-ray diffraction (XRD) patterns of the TiO₂ NFs and TiO₂ NFs-Ni are shown in Fig. 3. As observed in Fig. 3, TiO₂ NFs show six reflection peaks appeared at $2\theta = 25.4$ (101), 37.9 (004), 48.0 (200), 54.8 (105), 55.4 (211) and 63.8 (112), respectively, which were attributed to the anatase TiO₂. The diffraction peaks of the TiO₂ nanofibers were sharp and intense, indicating the highly crystalline character of the nanofibers. To verify whether Ni (NPs) was deposited to TiO₂ NF during the electrochemical process, XRD patterns of the TiO₂ (NF)-Ni (NPs) and TiO₂ (NFs) were recorded and compared. The diffraction peaks at 51.5° corresponded to the (2 0 0) facets of the Ni crystal, respectively [48].

Electrocatalytic Effect of TNF-NiNPs for Oxidation of Urea

The cyclic voltammetric (CV) behavior of the prepared electrode (TNF-NiNPs/GC) in 1.0 M NaOH solution is shown in Fig. 4. The impression of scanning rates on the CV response of the prepared electrode showed peak current increased with an increase in scanning rates and this pair of peaks is due to the oxidation of Ni(OH)₂ to NiOOH with this reaction [49-51]:



Both anodic and cathodic peak currents exhibited a linear response to the scan rates ranging from 0.02-0.4 V s⁻¹, inset (A) Fig. 4. This can be attributed to the immobilized redox couple on the surface with a surface-controlled process [52]. The surface coverage Γ^* can be calculated according to this equation [53]:

$$I_p = n^2 F^2 A \nu \Gamma^* / 4RT \quad (3)$$

where Γ^* is the surface coverage of redox species, n is the number of transferred electrons (1 for Ni²⁺/Ni³⁺), ν is the scan rate, A is the surface area of the electrode, all other symbols have their conventional meanings. The surface coverage of TNF-NiNPs /GC electrode was calculated to be $\Gamma_a^* = 4.16 \times 10^{-7}$ mol cm² for anodic peak currents, which is higher than corresponding value reported for the urea biosensor using Ni matrix [54].

Figure 5 shows the CV responses for the electrochemical oxidation of 0.2 M urea at the TNF-NiNPs/GC in 1.0 M NaOH phosphate buffer solution (pH 4.0) (curve c), curves (a) and (b) are the voltammograms of TNF-NiNPs/GC and bare GCE, respectively, curve (a) in 1.0 M NaOH phosphate buffer solution (pH 4.0), curve (b) bare GCE in 1.0 M NaOH phosphate buffer solution with 0.2 M urea. Inset shows the voltammograms c and b. It can be seen that the current of catalyst in 0.2 M urea at scan rate of 100 mV s⁻¹ is higher than other electrodes. This indicates that the TNF-NiNPs/GC catalyst can oxidize urea. The enhanced electrocatalytic activity of TNF-NiNPs /GC is due to the nanofibrous morphology increase the activity. Although, the specific surface area of the nanoparticles is higher than that for nanofibers, but the big axial ratio of the nanofibers increases the electrons transfer via the catalyst material which results in improvement of the electrocatalytic process [32].

The chronoamperometry method was used for comparison of the effect of different electrodes in urea oxidation. Figure 6 shows the results of chronoamperometry measurements of TNF-NiNPs/GC in 1 M NaOH and 0.2 M urea (a), TNF-NiNPs/GC in 1 M NaOH (b), GC in 1 M NaOH and 0.2 M urea (c), GC in 1 M NaOH (d). Results showed that the TNF-NiNPs/GC in 1 M NaOH and 0.2 M urea electrode have a superior current in comparison with other electrodes during the measurements. This is due to the

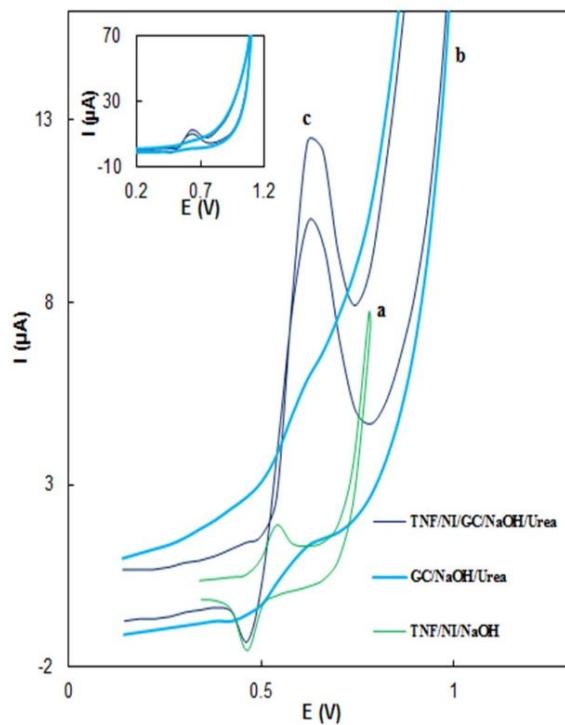


Fig. 5. CVs of the T (NF)-NiNPs/GC in 1 M NaOH (a), GC in 1 M NaOH and 0.2 M urea (b), T (NF)-NiNPs/GC in 1 M NaOH and 0.2 M urea (c), scan rate 100 mV s^{-1} .

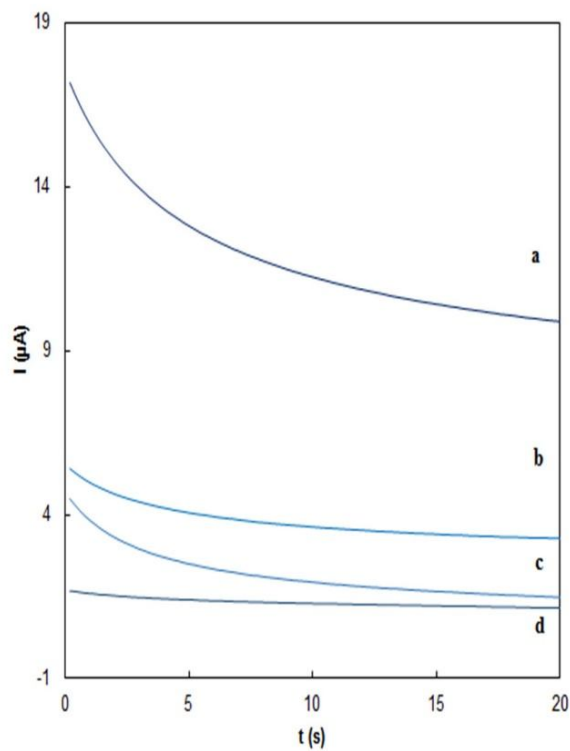


Fig. 6. Chronoamperograms of T (NF)-NiNPs/GC in 1 M NaOH and 0.2 M urea (a), T (NF)-NiNPs/GC in 1 M NaOH (b), GC in 1 M NaOH and 0.2 M urea (c) and GC in 1 M NaOH (d).

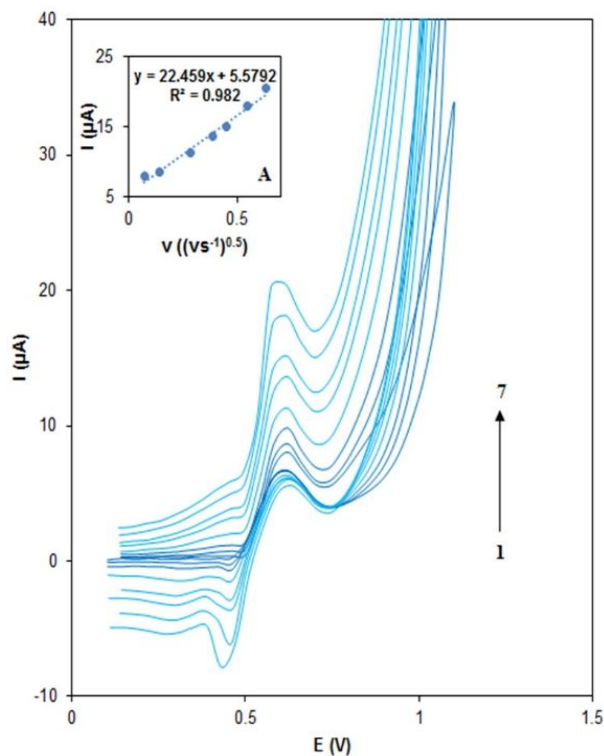


Fig. 7. CVs curves of the as-prepared T (NF)-NiNPs/GC electrode in 1 M NaOH solution in the presence of 0.2 M urea at different scan rates: 0.005, 0.02, 0.04, 0.08, 0.1, 0.2, 0.3 and 0.4 V s⁻¹ from 1 to 7, respectively, inset A the corresponding plot of peak current I_p vs. potential sweep rate $v^{1/2}$.

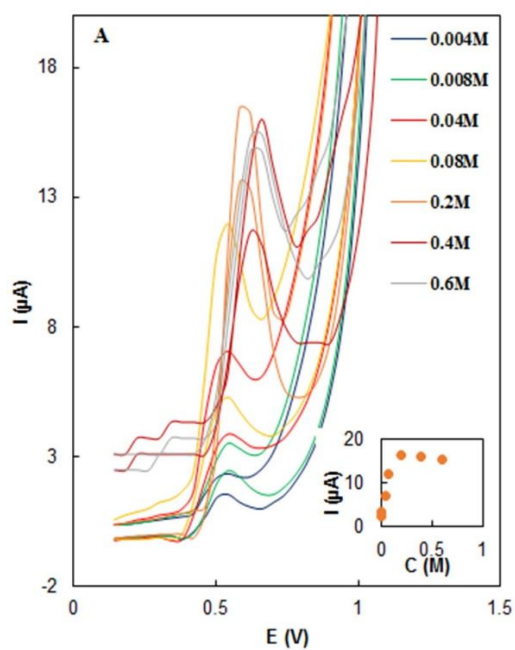


Fig. 8. Cyclic voltammograms for the prepared T (NF)-NiNPs/GC at different urea concentration: 0.004, 0.008, 0.04, 0.08, 0.2, 0.4 and 0.6 M urea in 1.0 M NaOH at scan rate 50 mV s⁻¹ and 25 oC. Inset A Plots of anodic peak current *versus* different concentration of urea.

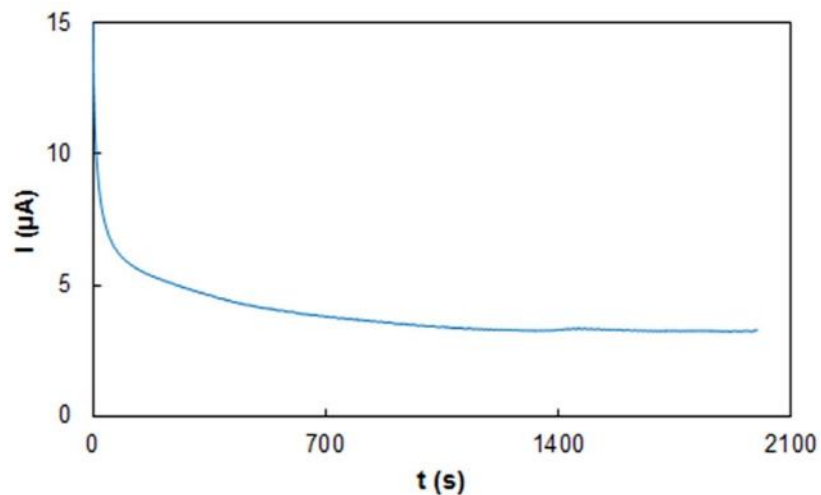


Fig. 9. Chronoamperometric analysis of TNF-NiNPs/GC electrode for study of the steady state behavior of urea oxidation containing 1 M NaOH and 0.2 M urea, within proximate 2000 s.

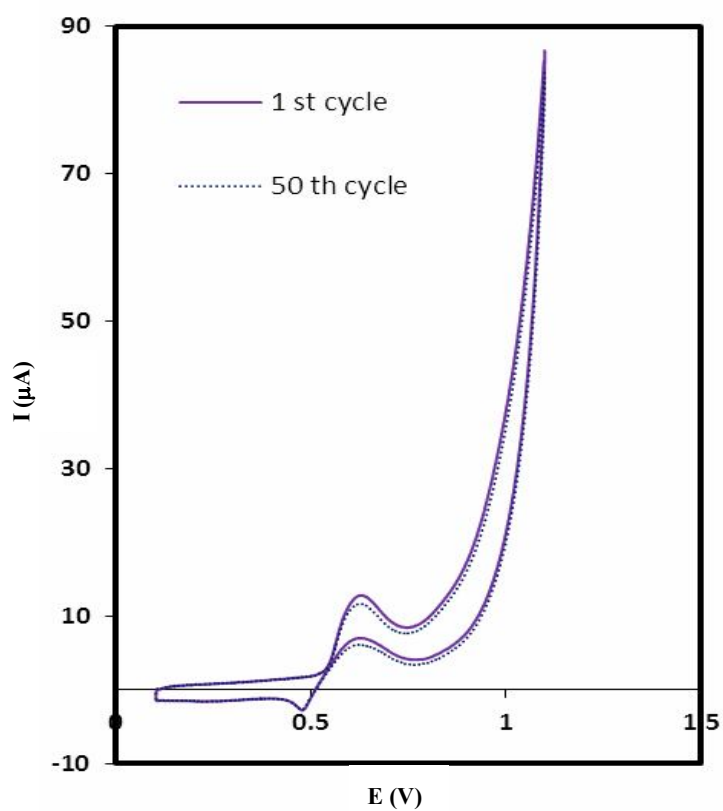


Fig. 10. 1st cycle and 50th cycle of TNF-NiNPs/GC electrode in 2 M Urea containing 1 M NaOH.

electrocatalytic properties of nanofibers in the T (NF)-Ni/GC electrode for urea oxidation, which is in according to the results of cyclic voltammetry of urea oxidation.

Figure 7 shows the effect of the scan rate on the electrocatalytic activity of 0.2 M urea by T (NF)-NiNPs/GC electrode in 1.0 M NaOH and in the range of 0.005-0.4 V s⁻¹. As shown, the anodic current increases with increasing the scan rate. As can be seen in Inset A, Fig. 7; plots of the anodic peak currents (I_p) were linearly dependent on $v^{1/2}$ in the range of 0.005-0.4 V s⁻¹; this linear relationship prove that the nature of the redox process was controlled by diffusion process.

CV was used for the investigation of different urea concentrations in 1 M NaOH and scan rate of 50 mV s⁻¹ Fig. 8. The strong electrocatalytic activity of the introduced nanofibers can be seen. Increasing the urea concentration in alkaline solution caused an increase in the anodic current. At low urea concentration, it could be considered that the increase in the anodic current is due to the diffusion controlled process. Although, after urea concentration of 0.2 M, anodic current decreases. Also the urea concentration does affect the anodic potential. This is due to the low oxidation of urea and the intermediates this means, adsorbed non oxidized urea or intermediates at the surface at high urea concentration need more over potential for oxidation [18]. And another anodic peak in the reverse scan in the urea oxidation region is because of the more oxidation of urea molecules due to regeneracy of the active (Ni²⁺/Ni³⁺) on the electrode surface which were coverage by intermediates, urea molecules or reaction products during the forward scan [18].

The long term stabilities and repeatability of the catalyst for urea oxidation containing 1 M NaOH and 0.2 M urea, were studied by employing steady state chronoamperometry under a constant voltage of 0.7 V and CV. In Fig. 9, it can be seen that the catalysts display high stability and after a quick initial decline it can be assigned to fast oxidation of urea molecules near to the electrode surface. Later on, the kinetic of urea oxidation reaction changes to be mass transfer-controlling process and electrode reach a steady-state Faradic current response within proximate 2000 s.

By CV, the peak separation of TNF-NiNPs/GC electrode after 50 cycles of cycling, stay unchanged and the

currents decreased by less than 3.7%. It can be concluded that the TNF-NiNPs/GC electrode has excellent electrochemical stability Fig. 10.

CONCLUSIONS

In this work, new construction procedure for urea oxidation based on Ni nanoparticles (NiNPs) decorated titanium dioxide (TiO₂) nanofibers (NFs) is reported. Results indicated that the effect of nanofibers increases the electrocatalytic activity toward urea oxidation in alkaline medium due to the synergetic influence and the nanofibrous morphology, the big axial ratio of the nanofibers increases the electrons transfer *via* the catalyst material. TiO₂ nanofibers are impressive and resistant electrocatalyst for urea oxidation and they are good support for electrodeposit of NiNPs. This work creates new idea to synthesize more effective nanofibers to be applied in urea oxidation process.

ACKNOWLEDGEMENTS

The authors wish to thank the Yazd University Research Council, IUT Research Council and Excellence in Sensors for financial support of this research.

REFERENCES

- [1] T. Trindade, P. O'Brien, N.L. Pickett, *Chem. Mater.* 13 (2001) 3843.
- [2] A.P. Alivisatos, *J. Phys. Chem.* 100 (1996) 13226.
- [3] M. Mazloum-Ardakani, A. Khoshroo, N. Taghavinia, L. Hosseinzadeh, *RSC Adv.* 6 (2016) 12537.
- [4] Y. Cho, W.H. Lee, H. Kim, *J. Electrochem. Soc.* 164 (2017) F65.
- [5] M. Mazloum-Ardakani, A. Khoshroo, *Electrochim. Acta* 130 (2014) 634.
- [6] M. E. Unates, M.E. Folquer, J.R. Vilche, A.J. Arvia, *J. Electrochem. Soc.* 139 (1992) 2697.
- [7] M. Mazloum-Ardakani, E. Amin-Sadrabadi, A. Khoshroo, *J. Electroanal. Chem.* 775 (2016) 116.
- [8] C.M. Welch, R.G. Compton, *Anal. Bioanal. Chem.* 384 (2006) 601.
- [9] A.L. Rinaldi, S. Sobral, R. Carballo, *Electroanalysis*

- 29 (2017) 1961.
- [10] S.N.S. Goubert-Renaudin, A. Wieckowski, J. Electroanal. Chem. 652 (2011) 44.
- [11] M. Jafarian, M. Babae, F. Gobal, M.G. Mahjani, J. Electroanal. Chem. 652 (2011) 8.
- [12] L. Bian, Q. Du, M. Luo, L. Qu, M. Li, Int. J. Hydrogen Energy 42 (2017) 25244.
- [13] F. Yang, K. Cheng, K. Ye, X. Xiao, F. Guo, J. Yin, G. Wang, D. Cao, Electrochim. Acta 114 (2013) 478.
- [14] B.K. Boggs, R.L. King, G.G. Botte, Chem. Commun. 4859 (2009).
- [15] F. Bedioui, A. Ordaz, S.J. Ferrer, S. Gutie, 70 (2003).
- [16] A.T. Miller, B.L. Hassler, G.G. Botte, J. Appl. Electrochem. 42 (2012) 925.
- [17] R.L. King, G.G. Botte, J. Power Sources 196 (2011) 2773.
- [18] V. Vedharathinam, G.G. Botte, Electrochim. Acta 81 (2012) 292.
- [19] V. Vedharathinam, G.G. Botte, Electrochim. Acta 108 (2013) 660.
- [20] D. Wang, W. Yan, S.H. Vijapur, G.G. Botte, J. Power Sources 217 (2012) 498.
- [21] K. Ye, D. Zhang, F. Guo, K. Cheng, G. Wang, D. Cao, J. Power Sources 283 (2015) 408.
- [22] F. Guo, K. Ye, K. Cheng, G. Wang, D. Cao, J. Power Sources 278 (2015) 562.
- [23] W. Yan, D. Wang, L.A. Diaz, G.G. Botte, Electrochim. Acta 134 (2014) 266.
- [24] J.-C. Chen, J.-C. Chou, T.-P. Sun, S.-K. Hsiung, Sensors Actuators B Chem. 91 (2003) 180.
- [25] C.-P. Huang, Y.-K. Li, T.-M. Chen, Biosens. Bioelectron. 22 (2007) 1835.
- [26] A. Maaref, H. Barhouni, M. Rammah, C. Martelet, N. Jaffrezic-Renault, C. Mousty, S. Cosnier, Sensors Actuators B Chem. 123 (2007) 671.
- [27] M. Vidotti, M.R. Silva, R.P. Salvador, S.I.C. de Torresi, L.H. Dall'Antonia, Electrochim. Acta 53 (2008) 4030.
- [28] C.C. Jara, S. Di Giulio, D. Fino, P. Spinelli, J. Appl. Electrochem. 38 (2008) 915.
- [29] W. Simka, J. Piotrowski, A. Robak, G. Nawrat, J. Appl. Electrochem. 39 (2009) 1137.
- [30] B.J. Hernlem, Water Res. 39 (2005) 2245.
- [31] R. Lan, S. Tao, J.T.S. Irvine, Energy Environ. Sci. 3 (2010) 438.
- [32] N.A.M. Barakat, M.H. El-Newehy, A.S. Yasin, Z.K. Ghouri, S.S. Al-Deyab, Appl. Catal. A Gen. 510 (2016) 180.
- [33] S. Huang, Y. Ding, Y. Liu, L. Su, R. Filosa, Y. Lei, Electroanalysis 23 (2011) 1912.
- [34] I.-D. Kim, A. Rothschild, B.H. Lee, D.Y. Kim, S.M. Jo, H.L. Tuller, Nano Lett. 6 (2006) 2009.
- [35] M. Bahram, S. Salami, M. Moghtader, P. Najafi Moghadam, A. Reza Fareghi, M. Rasoli, S. Salimpoor, Anal. Bioanal. Chem. Res. 4 (2017) 53.
- [36] H. Yoon, J. Jang, Adv. Funct. Mater. 19 (2009) 1567.
- [37] S.R. Hosseini, S. Ghasemi, M. Kamali-rousta, Int. J. Hydrogen Energy 2 (2016).
- [38] A. Stafiniak, B. Boratyński, A. Baranowska-Korczyn, A. Szyszka, M. Ramiączek-Krasowska, J. Prazmowska, K. Fronc, D. Elbaum, R. Paszkiewicz, M. Tłaczała, Sensors Actuators B Chem. 160 (2011) 1413.
- [39] N.A.M. Barakat, M.A. Yassin, A.S. Yasin, Int. J. Hydrogen Energy 1 (2017).
- [40] H. Tang, F. Yan, Q. Tai, H.L.W. Chan, Biosens. Bioelectron. 25 (2010) 1646.
- [41] S. Bao, C.M. Li, J. Zang, X. Cui, Y. Qiao, J. Guo, Adv. Funct. Mater. 18 (2008) 591.
- [42] K. Mondal, M.A. Ali, V.V. Agrawal, B.D. Malhotra, A. Sharma, ACS Appl. Mater. Interfaces 6 (2014) 2516.
- [43] Q. Kang, L. Yang, Q. Cai, Bioelectrochemistry 74 (2008) 62.
- [44] M. Mazloun-Ardakani, A. Khoshroo, Anal. Chim. Acta 798 (2013) 25.
- [45] L. Larrondo, R.S.T.J. Manley 19 (1981) 909.
- [46] M. Mazloun-Ardakani, M. Yavari, A. Khoshroo, Electroanalysis 29 (2017) 231.
- [47] R. Das, B.K. Das, R. Shukla, T. Prabakaran, A. Shyam, Sadhana 37 (2012) 629.
- [48] Y. Ni, L. Jin, L. Zhang, J. Hong, J. Mater. Chem. 20 (2010) 6430.
- [49] M. Fleischmann, K. Korinek, D. Pletcher, J. Electroanal. Chem. Interfacial Electrochem. 31 (1971) 39.

- [50] M. Vuković, *J. Appl. Electrochem.* 24 (1994) 878.
- [51] R. Ostermann, D. Li, Y. Yin, J.T. McCann, Y. Xia, *Nano Lett.* 6 (2006) 1297.
- [52] J. Zhu, J. Jiang, J. Liu, R. Ding, Y. Li, H. Ding, Y. Feng, G. Wei, X. Huang, *Rsc Adv.* 1 (2011) 1020.
- [53] A.J. Bard, L.R. Faulkner, *Electrochem. Methods*, 2nd Ed.; Wiley New York, 2001.
- [54] M. Tyagi, M. Tomar, V. Gupta, *Biosens. Bioelectron.* 41 (2013) 110.